Supporting Information

Double-acceptors conjugated polymers for NIR-II fluorescence imaging and NIR-II photothermal therapy application

Chen Yan [a], Sun Bo [a], Jiang Xinyue [a], Yuan Zhangyu [a], Chen Shangyu [a], Sun Pengfei [*a], Fan Quli [*a] & Huang Wei [b]

[a] Key Laboratory for Organic Electronics and Information Displays & Institute of Advanced Materials, Jiangsu National Synergetic Innovation Center for Advanced Materials, Nanjing University of Posts & Telecommunications, Nanjing 210023, China;
[b] Frontiers Science Center for Flexible Electronics & Shaanxi Institute of Flexible Electronics, Northwestern Polytechnical University,Xi'an 710072, China

1. Experimental Section

1.1 Materials

3,6-bis(5-bromothiophen-2-yl)-2,5-bis(2-octyldodecyl)pyrrolo[3,4-*c*]pyrrole-1,4(2*H*,5*H*)-dione (DPP, 97%), 4,9-bis(bromothiophen-2-yl)-6,7-bis(4-(hexyloxy)phenyl)-[1,2,5]thiadiazolo[3,4-*g*]quinoxaline (TTQ, 97%), (4,4'-didodecyl-[2,2'-bithiophene]-5,5'-diyl)bis(trimethylstannane) (TC, 97%) were purchased from SunaTech Inc. Tris-(dibenzylideneacetone)dipalladium(0), triphenylphosphine were purchased from J&K Scientific Ltd. Methyl alcohol was purchased from NanJing WanQing Chemical Glassware Instrument Co., Ltd. The mPEG-DSPE was purchased from Sigma-Aldrich (Shanghai, China). All chemical materials were used without further purification. Besides, all synthetic experiments were conducted in the condition of anhydrous and Nitrogen protection. 4T1 cells were obtained from the Shanghai Laboratory Animal Center, Chinese Academy of Science (SLACCAS). The Annexin V-FITC/propidium iodide (PI) cell apoptosis kit, 3-(4,5-dimethylthiazol-2-yl)-2,5-diphenyl-tetrazolium bromide (MTT), Fetal bovine serum (FBS) and Phosphate buffer saline (PBS) were obtained from KeyGen Biological Technology Co., Ltd (Nanjing, China). Dulbecco's Modified Eagle's Medium (DMEM, Gibco, U.S.) was obtained from Gene Tech Co. (Shanghai, China).

1.2 Instrumentations Characterization

The ^{1}H NMR spectra were performed on a Bruker Ultra Shield Plus 400 MHz spectrometer at 298 K by choosing $CDCl_3$ as the solvent and tetramethylsilane (TMS) as the internal standard. Gel permeation chromatography (GPC), determining the number-average molecular weight (M_n) and polydispersity (PDI) of the polymers, was performed with THF as the eluent using Shim-pack GPC-80 X columns. The morphology of nanoparticles was observed by a transmission electron microscope (TEM, Hitachi HT7700), whose acceleration voltage is 100 KV. Dynamic light scattering (DLS) analysis was conducted on a commercial laser light scattering spectrometer (ALV-7004; ALV-GmbH, Langen, Germany) equipped with a multi-τ digital time correlator and a He-Ne laser (λ = 632.8 nm). The hydrodynamic diameters (D_h) data were extracted through a CONTIN analysis. All samples we used for the test were optically cleared by filtration via 0.45 μm Millipore filter. The scattering angle was set up to 90° and all tests were conducted under room temperature. A Shimadzu UV-3600 spectrophotometer was utilized to record the absorption spectra of our samples at room temperature. NIR-II fluorescence spectra were measured using an NIR-II spectrophotometer (Fluorolog 3, Horiba). NIR InGaAs was selected as the detector, with an excitation wavelength

of 808 nm obtained from a diode laser operating at 25.0 ± 0.5 °C. After the raw emission data were collected, the fluorescence signal was further confirmed and corrected for the sensitivity of InGaAs detector profile and output through the T1 channel. The laser was purchased from Changchun New Industries Optoelectronics Technology Co., Ltd. The *in vitro* and *in vivo* NIR-II FI experiments were conducted on an NIR-II fluorescence imaging system (Wuhan Grand-imaging Technology Co., Ltd) with different filter and two types of lenses (50 or 100 mm) under the 808 nm laser irradiation. A 640 × 512 pixel two-dimensional InGaAs array from Princeton Instruments in NIR-II fluorescence windows was equipped in this NIR-II FI system. All photothermal tests were detected using a Fotric 225 instrument (IR thermal camera, ± 2 °C) purchased from Fotric Co., Ltd (Shanghai, China). The methyl thiazolyl tetrazolium (MTT) analysis was conducted using a PowerWave XS/XS2 microplate spectrophotometer (BioTek, Winooski, VT). The flow cytometry experiments were performed using a Flow Sight Imaging Flow Cytometer (Merck Millipore, Darmstadt, Germany).

1.3 Synthesis of three polymers

1.3.1 *Preparation of P1*

4,9-bis(bromothiophen-2-yl)-6,7-bis(4-(hexyloxy)phenyl)-[1,2,5]thiadiazolo[3,4-*g*]quinoxaline (TTQ, 14.7 mg, 0.017 mmol), 3,6-bis(5-bromothiophen-2-yl)-2,5-bis(2-octyldodecyl)pyrrolo[3,4-*c*]pyrrole-1,4(2*H*,5*H*)-dione (DPP, 33.6 mg, 0.033 mmol), (4,4'-didodecyl-[2,2'-bithiophene]-5,5'-diyl)bis(trimethylstannane) (TC, 41.4 mg, 0.05mmol), triphenylphosphine ($Pd_2(dba)_3$, 0.5 mg, 0.0016 mmol), tris-(dibenzylideneacetone)dipalladium(0) ($P(o\text{-}Tol)_3$, 2 mg, 0.00218 mmol) and anhydrous toluene (2.5 mL) were added into a 10 mL polymer tube, and the system was degassed and filled with argon for 20-30 min. Then the reaction mixture was reacted in an oil bath at 100 °C and stopped when the color of the reaction solution changes from black green to brown red. After cooling to room temperature, the polymerization mixture was poured and stirred in 50 mL of methanol solution. Then, the polymer precipitated out as a black solid and subsequently was filtered with a filter paper.

1.3.2 *Preparation of P2*

4,9-bis(bromothiophen-2-yl)-6,7-bis(4-(hexyloxy)phenyl)-[1,2,5]thiadiazolo[3,4-*g*]quinoxaline (TTQ, 21.6 mg, 0.025 mmol), 3,6-bis(5-bromothiophen-2-yl)-2,5-bis(2-octyldodecyl)pyrrolo[3,4-*c*]pyrrole-1,4(2*H*,5*H*)-dione (DPP, 25.5 mg, 0.025 mmol), (4,4'-didodecyl-[2,2'-bithiophene]-5,5'-diyl)bis(trimethylstannane) (TC, 41.4 mg, 0.05 mmol), triphenylphosphine ($Pd_2(dba)_3$, 0.5 mg, 0.0016 mmol), tris-(dibenzylideneacetone)dipalladium(0) ($P(o\text{-}Tol)_3$, 2 mg, 0.00218 mmol) and anhydrous toluene (2.5 mL) were added into a 10 mL polymer tube, and the system was degassed and filled with argon for 20-30 min. Then the reaction mixture was reacted in an oil bath at 100 °C and stopped when the color of the reaction solution changes from black green to brown red. After cooling to room temperature, the polymerization mixture was poured and stirred in 50 mL of methanol solution. Then, the polymer precipitated out as a black solid and subsequently was filtered with a filter paper.

1.3.3 *Preparation of P3*

4,9-bis(bromothiophen-2-yl)-6,7-bis(4-(hexyloxy)phenyl)-[1,2,5]thiadiazolo[3,4-*g*]quinoxaline (TTQ, 28.5 mg, 0.033 mmol), 3,6-bis(5-bromothiophen-2-yl)-2,5-bis(2-octyldodecyl)pyrrolo[3,4-*c*]pyrrole-1,4(2*H*,5*H*)-dione (DPP, 17.3 mg, 0.017 mmol), (4,4'-didodecyl-[2,2'-bithiophene]-5,5'-diyl)bis(trimethylstannane) (TC, 41.43 mg, 0.05mmol), triphenylphosphine ($Pd_2(dba)_3$, 0.5 mg, 0.0016 mmol), tris-(dibenzylideneacetone)dipalladium(0) ($P(o\text{-}Tol)_3$, 2 mg, 0.00218 mmol) and anhydrous toluene (2.5 mL) were added into a 10 mL polymer tube, and the system was degassed and filled with argon for 20-30 min. Then the reaction mixture was reacted in an oil bath at 100 °C and stopped when the color of the reaction solution changed from black green to brown red. After cooling to room temperature, the polymerization mixture was poured and stirred in 50 mL of methanol solution. Then, the polymer precipitated out as a black solid and subsequently was filtered with a filter paper.

1.4 Fabrication of nanoparticles based on conjugated polymers

Three nanoparticles (P1 NPs, P2 NPs, and P3 NPs) were prepared by a conventional nanoprecipitation method with amphiphilic 1,2-distearoylsn-glycero-3- phosphoethanolamine- polyethylene glycol-5000 (mPEG-DSPE) as the

carrier. They were prepared according to the following procedure. First, each of the three conjugated polymers (P1, P2, and P3) was dissolved in anhydrous tetrahydrofuran (THF). The THF solution was then rapidly injected into deionized water containing mPEG-DSPE under vigorous sonication. Finally, THF was evaporated, and P1 NPs, P2 NPs, and P3 NPs were obtained.

1.5 Photostability

The Photodynamics of nanoparticles aqueous solutions in PBS, DMEM and FBS were determined by near-infrared two-region fluorescence spectrometer. Firstly, 1 mL nanoparticles solution (0.1 mg mL^{-1}) was mixed with 1 mL PBS buffer solution, FBS minimum essential Medium and DMEM (Dulbecco's Minimum Essential Medium), respectively, and then the corresponding photodynamics was determined by continuous irradiation with 808 nm laser for 1 h. Finally, the fluorescence intensity of the maximum peak was plotted as a function of time.

1.6 Fluorescent Quantum Yield

The fluorescence quantum yield (QY) of three conjugated polymers (P1, P2, and P3) and three nanoparticles (P1 NPs, P2 NPs, and P3 NPs) were measured by the previous method. The QYs were determined according to the reference fluorophore IR 1061, as a reference sample, which has a QY value of 1.7 ± 0.5% in THF. Five different concentrations around or less than an OD of 0.1 were measured, and all samples were analyzed at 25 °C. Their QYs were calculated by the following equation:

$$QY(sample) = QY(ref) * \frac{slope(sample)}{slope(ref)} * \frac{n^2(sample)}{n^2(ref)} \quad (1)$$

The parameter n is the refractive index of solvent. The slopes are the slopes of the linear curves of the integrated fluorescence intensity against the absorption.

1.7 *In vitro* photothermal effect and photothermal conversion efficiency

To evaluate the photothermal effect of the three nanoparticles, 100 μL of three nanoparticle solutions with concentrations of 0.1 and 0.04 mg mL^{-1} were successively irradiated with 1064 nm laser (1.0 W cm^{-2}, 7 min). The temperature changes of the three nanoparticle solutions were performed with an IR thermal camera, and these data were recorded every 30 s.

As we all known, the nature of photothermal therapy is that photothermal agents having the inherent ability to absorb NIR light convert NIR laser energy into heat. Hence, it is important to first explore the photothermal conversion efficiency (ŋ) of the NPs. To study the photothermal conversion behavior of P1 NPs, a thermal imaging camera (Fotric 225, Fotric Precision Instruments, USA, ± 2 °C) was used to perform the thermal imaging of NPs in an aqueous solution. First, an aqueous solution of nanoparticles (0.1 mg mL^{-1}) was configured, 100 μL of which was added into a 200 μL centrifuge tube. The temperature changes of a fixed concentration of NPs (0.1 mg mL^{-1}) were irradiated with a 1064 nm laser (1.0 W cm^{-2}, 8 min), and then the laser was shut off. Finally, we can obtain a temperature increase and drop curve.

The photothermal conversion efficiency (ŋ) was calculated using equations (1) and (2) expressed below. The photothermal conversion efficiency of the P1 NPs was determined to be through the collected data and equation.

$$ŋ = [hS(T_{max}-T_{suur})-Q_{dis}]/[I(1-10^{-A_{1064}})] \quad (1)$$

$$\tau_s = m_D C_D/hS \quad (2)$$

The parameters S, h, T_{max}, T_{surr}, Q_{dis}, I and A_{1064} are the container's surface area, heat-transfer coefficient, maximum laser-trigger temperature, indoor temperature, heat dissipation caused by the light absorbing of quartz cuvette, intensity of laser (1.0 W cm^{-2}) and absorbance of P1 NPs at 1064 nm, respectively.

Parameter τ_s is the time constant of the sample system. The parameters m_D and C_D are the mass and heat capacity of the solvent, respectively.

1.8 Cells Culture and *in vitro* Cytotoxicity Assay

4T1 cells were cultured in DMEM with 10% fetal bovine serum. And cells were maintained at 37 °C and 5% CO_2 conditions.

The 4T1 cells were used for the *in vitro* cytotoxicity assessment of P1 NPs by MTT assays. First, cells, seeded 2 × 10^4 peer well, were cultured in DMEM in 96-well plates at 37 °C and 5% CO_2 condition for 24 h. The medium was then replaced by the mixture of the fresh DMEM medium and different concentrations of P1 NPs (0, 2.5, 5, 10, 20, and 40 μg mL^{-1}). Subsequently the cells were further cultured in a dark environment for 48 h. Afterward, the medium was replaced by 100 μL of fresh DMEM medium, and subsequently the 20 μL of MTT (5 mg mL^{-1}) was added to each well. Finally, after 4 h of incubation, the upper supernatant was aspirated, and 100 μL of DMSO was added to each well. Cell viability was calculated by the absorbance at 490 nm by a PowerWave XS/XS2 microplate spectrophotometer.

1.9 *In vitro* Cellular Uptake

The 4T1 cells were also used for the assessment of cellular uptake. First, cells, seeded 4 × 10^4 peer well, were incubated in DMEM in a 6-well plate at 37 °C and 5% CO_2 condition for 24 h. Subsequently, the medium was replaced by one of the two groups, including 1 mL fresh DMEM medium alone and the 1mL mixture of fresh DMEM medium and P1 NPs (0.04 mg mL^{-1}), respectively. The treated cells were further incubated at 37 ^oC and 5% CO_2 condition for 12 h. Afterward, the upper supernatant was sucked out and 500 μL of PBS was added to clean twice and remove dead cells. Subsequently, PBS was removed and EDTA was added, and the cells were dissolved in an incubator at 37 °C and 5% CO_2 for 7 min. Later 1 mL of DMEM was added and the cells were transferred into a 15 mL centrifuge tube and centrifuged for 3 min. The supernatant was then removed, and 100 μL of PBS was added to the centrifuge tube. Finally, the cells were transferred to a 96-well plate, where NIR-II fluorescence images of the two groups were captured under the 808 nm laser excitation with a 1064 LP filter, which demonstrated the *in vitro* cellular uptake ability of the P1 NPs.

1.10 *In vitro* Photocytotoxity Assay

The 4T1 cells were used for the *in vitro* cytotoxicity assessment of P1 NPs by MTT assays. First, cells, seeded at 2 × 10^4 cells/well, were cultured in DMEM in 96-well plates at 37 °C and 5% CO_2 condition for 24 h. Then, the medium was replaced by a mixture of fresh DMEM medium and different concentrations of P1 NPs (0, 2.5, 5, 10, 20, and 40 μg mL^{-1}), following which the selected wells (P1 NPs + laser group) were irradiated under 1064 nm laser illumination (1.0 W cm^{-2}) for 5 min and further incubated at 37 °C and 5% CO_2 for 24 h. The P1 NPs treated wells (P1 NPs group) were not irradiated with 1064 nm laser illumination. Afterwards, the medium was replaced with 100 μL of fresh DMEM medium, and 20 μL of MTT (5 mg mL^{-1}) was added to each well. Finally, after 4 h of incubation, the upper supernatant was removed, and 100 μL of DMSO was added. Cell viability was calculated by measuring the absorbance at 490 nm using a PowerWave XS/XS2 microplate spectrophotometer.

1.11 Assessment of Photothermal Effect *in vitro* by Confocal Imaging and Flow Cytometry

The 4T1 cells were used for the assessment of the photothermal effect by confocal imaging. Firstly, the 4T1cells were cultured with DMEM in CLSM culture dishes (Costar) until the cell density increased to 1 × 10^5 cells mL^{-1} per

well. Subsequently, the medium was replaced with a mixture medium (40 μg mL^{-1}) of the fresh DMEM medium and P1 NPs. The selected wells were then irradiated with or without the 1064 nm laser illumination (1.0 W cm^{-2}, 5 min), respectively. After 24 h of apoptosis, the cells were washed twice to remove the cell debris and were then incubated with calcein- AM/propidium iodide (PI) dye solution for 10 min. Finally, the cells were imaged using CLSM (Olympus Fluoview FV1000, Olympus Corp., Japan).

The 4T1 cells were used for the assessment of the photothermal effect by flow cytometry. First, the 4T1 cells were cultured with DMEM in 6-well plates until the cell density increased to 1 × 10^5 cells mL^{-1} per well. The medium was then replaced with a mixture medium of fresh DMEM medium and P1 NPs (40 μg mL^{-1}). Subsequently, the selected wells were irradiated with or without the 1064 nm laser illumination (1.0 W cm^{-2}, 5 min), respectively. After 24 h of apoptosis, the wells underwent two iterations of supernatant removal and the 500 μL PBS addition to remove dead cells. The PBS was then removed and EDTA was added, and the cells were dissolved in an incubator at 37 °C and 5% CO_2 condition for 7 min. Later, 1 mL of DMEM was added, and the cells were transferred into a 15 mL centrifuge tube. After the cells were centrifuged for 3 min, the supernatant was removed, Annexin V-FITC/PI dye solution was added to the collected cells for staining, and the cells were tested by flow cytometry.

1.12 The Penetration depth of P1 NPs

The penetration depth of P1 NPs was measured to assess the tissue penetration depth. First, P1 NPs with a concentration of 2 mg mL^{-1} was configured. Subsequently, a fresh frozen chicken breast was sectioned with a width of 4 × 4 × 2 as the base, and then cut into chicken pieces with different thickness (1, 2, 4, 6, and 8 mm). Then, 2 mg mL^{-1} P1 NPs aqueous solution was injected into the tubes of Stama Cells PE of 1 mm diameter with the thin tubes placed on the chicken blocks. This setup was placed in the NIR-II fluorescence imaging system. While the thin tubes were covering with chicken slices of different thicknesses, the NIR-II fluorescence imaging image intensities were measured by the analysis software in the instrument.

1.13 Animal model

All experiments using animals were performed according to the specifications of The National Regulation of China for Care and Use of Laboratory Animals, and the protocol was approved by the Jiangsu Administration of Experimental Animals. 4T1 tumor-bearing mice (age 5-6 weeks) were obtained from the Jiangsu Kaiji Biotechnology Co., LTD. 4T1 tumors were planted by hypodermic injection of suspension of 4T1 cells into the right armpit of mice. The tumor volume was calculated as the following equation:

$$V=0.5\ LW^2 \quad (1)$$

The parameter L and W are the longitudinal and transverse diameters of the tumor, respectively.

1.14 *In vivo* NIR-II Fluorescence Imaging of Vascular system and Tumor

For further biological applications, NIR-II fluorescence images of the vascular system (including the body, hind limb, and belly vessel) and tumor were captured using the NIR-II fluorescence imaging system. When the average tumor volume of 4T1 tumor-bearing mice reached approximately 100 mm^3, the mice were intravenously injected with P1 NPs solution (100 μL, 2 mg mL^{-1}). The mice were then anesthetized, following which the comatose mice were fixed upside down in the NIR-II fluorescence imaging system. The NIR-II fluorescence imaging of the entire body and the vasculatures of the hind limb and belly vessel were performed under the 808 nm laser excitation with 1064 nm LP filter. Subsequently, these images of the vasculatures of the hind limb and belly vessel were processed using Image J software to obtain their corresponding full width at half maximum (FWHM) and signal background ratio (SBR). Meanwhile, real-time *in vivo* NIR-II fluorescence imaging was performed at different post-injection times under the 808 nm laser excitation with 1064 nm LP filter. Finally, the NIR-II fluorescence signal intensity of NIR-II images was measured using the NIR-II in vivo imaging system software.

In addition, to examine the biodistribution of P1 NPs, 4T1 tumor-bearing mice were sacrificed on 48 h post injection of P1 NPs. The tumor and the main organs (heart, liver, spleen, lung, and kidney) were excised and subsequently placed in the NIR-II fluorescence system. Their images were captured with 1064 LP filter under the 808 nm laser excitation. It was found that the strong NIR-II fluorescence signal was mainly observed in the tumor, liver and spleen.

1.15 *In vivo* Photothermal therapy (PTT)

When the average tumor volume of 4T1 tumor-bearing mice reached approximately 100 mm^3, the mice were randomly divided into four groups (five mice per group). Two groups of mice were administered with PBS intravenously, while the other groups of mice were intravenously injected with P1 NPs (100 μL, 2 mg mL^{-1}). Two groups of mice injected with PBS were treated with or without 1064 nm laser illumination, so do the other groups of mice injected with P1 NPs. When the mice of the two groups irradiated by the 1064 nm laser excitation were intravenously injected for 24 h, they were anesthetized and subsequently exposed to the 1064 nm laser on the tumor site for 5 min with a power density of 1.0 W cm^{-2}. In addition, the temperature changes of the tumor sites were recorded, and *in vivo* photothermal images were captured. Afterwards, these mice were housed under SPF conditions. Tumor size, tumor weight, and body weight were monitored and measured every two days. At 15 days, these mice were sacrificed, and the tumors were collected. The collected tumors were fixed in 4% neutral-buffered paraformaldehyde and embedded in paraffin for hematoxylin-eosin (H&E) staining, and the images of the histological tumor sections were obtained.

2. Figures

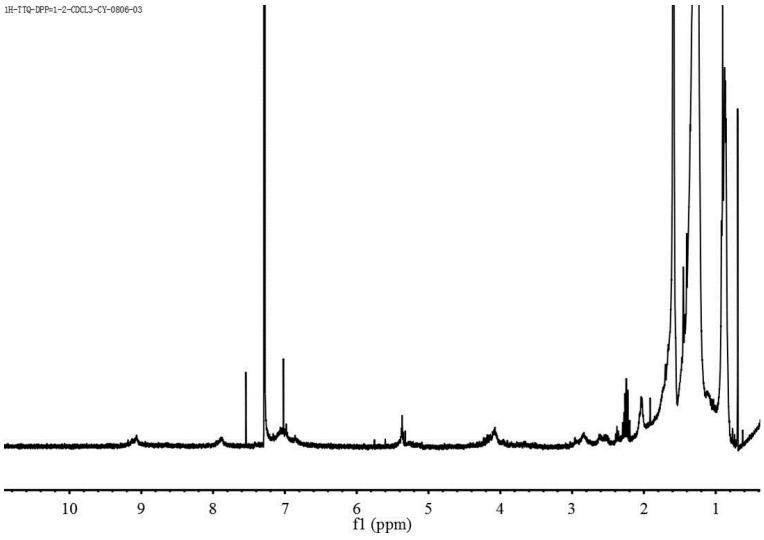

Fig. S1 ^1H NMR spectrum of P1 in $CDCl_3$.

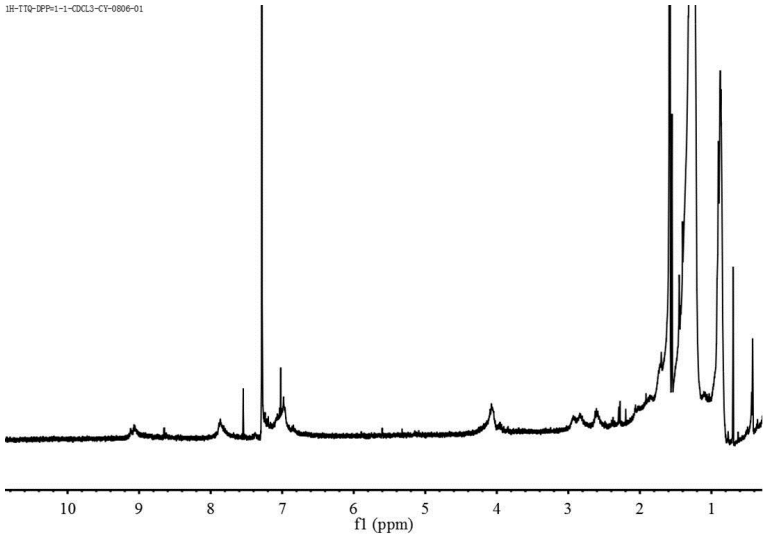

Fig. S2 ^{1}H NMR spectrum of P2 in $CDCl_3$.

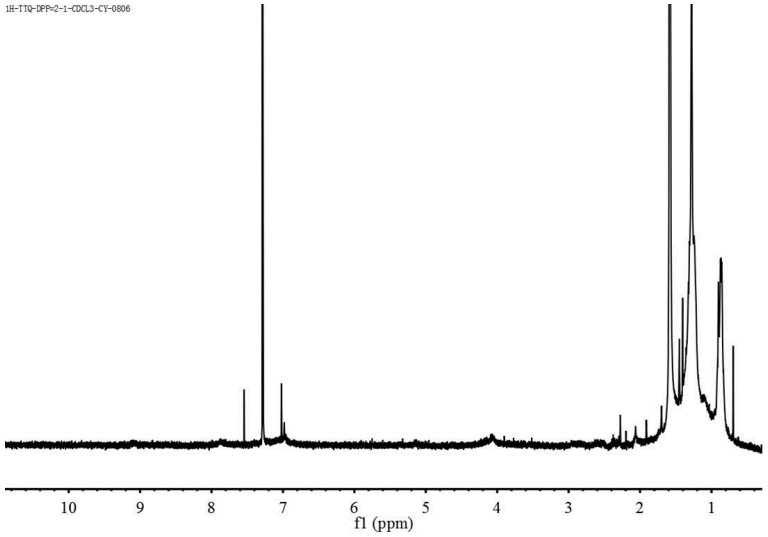

Fig. S3 ^{1}H NMR spectrum of P3 in $CDCl_3$.

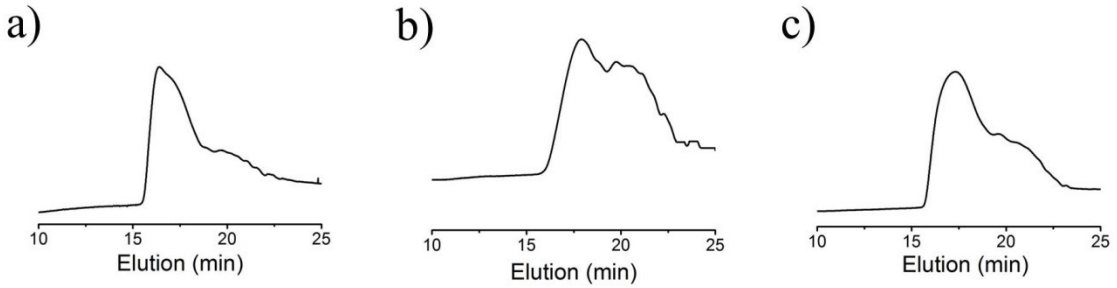

Fig. S4 GPC spectra of (a) P1, (b) P2, and (c) P3 in THF.

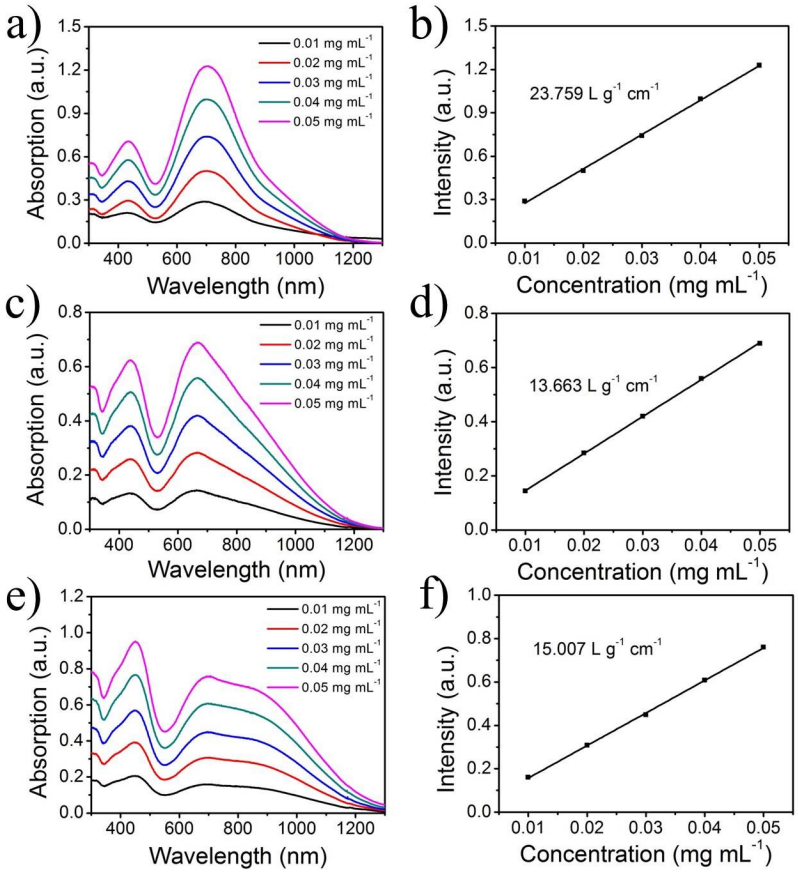

Fig. S5 Photophysical performances of three conjugated polymers: UV-vis-NIR absorption spectra of (a) P1, (c) P2 and (e) P3 in THF at different concentrations. (b), (d) and (f) were their extinction coefficients at their corresponding maximum absorption peaks, respectively.

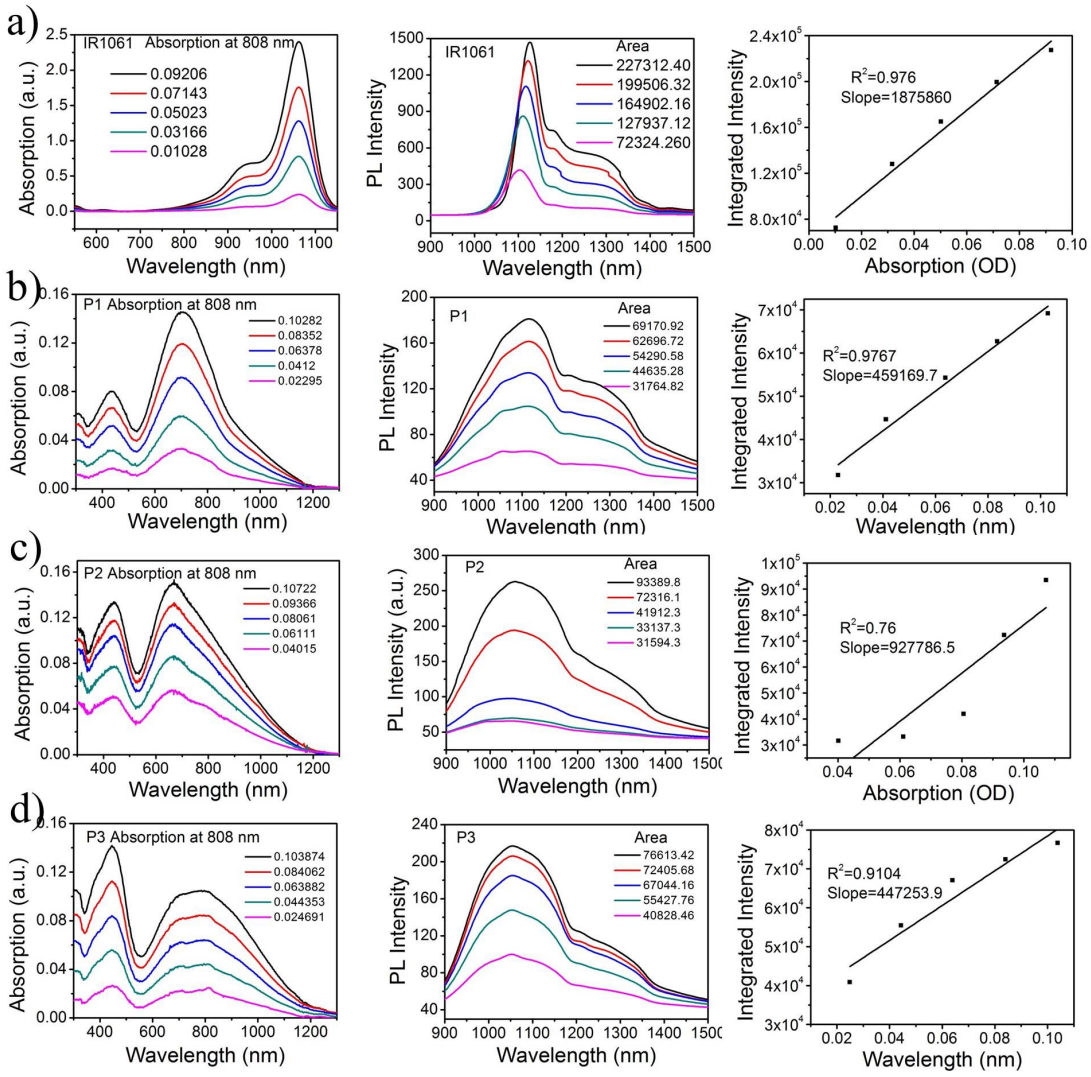

Fig. S6 Fluorescent quantum yield measurement of (b) P1, (c) P2, and (d) P3 with IR 1061 (a) as the reference sample. On the left is their corresponding absorption spectrum of P1, P2, and P3 in THF and IR 1061 in DCM at different absorption. The middle figures are their corresponding fluorescence emission spectra of P1, P2, and P3 in THF at different absorption. On the right is the plot of the integrated intensity of IR 1061 in DCM, P1, P2, and P3 in THF.

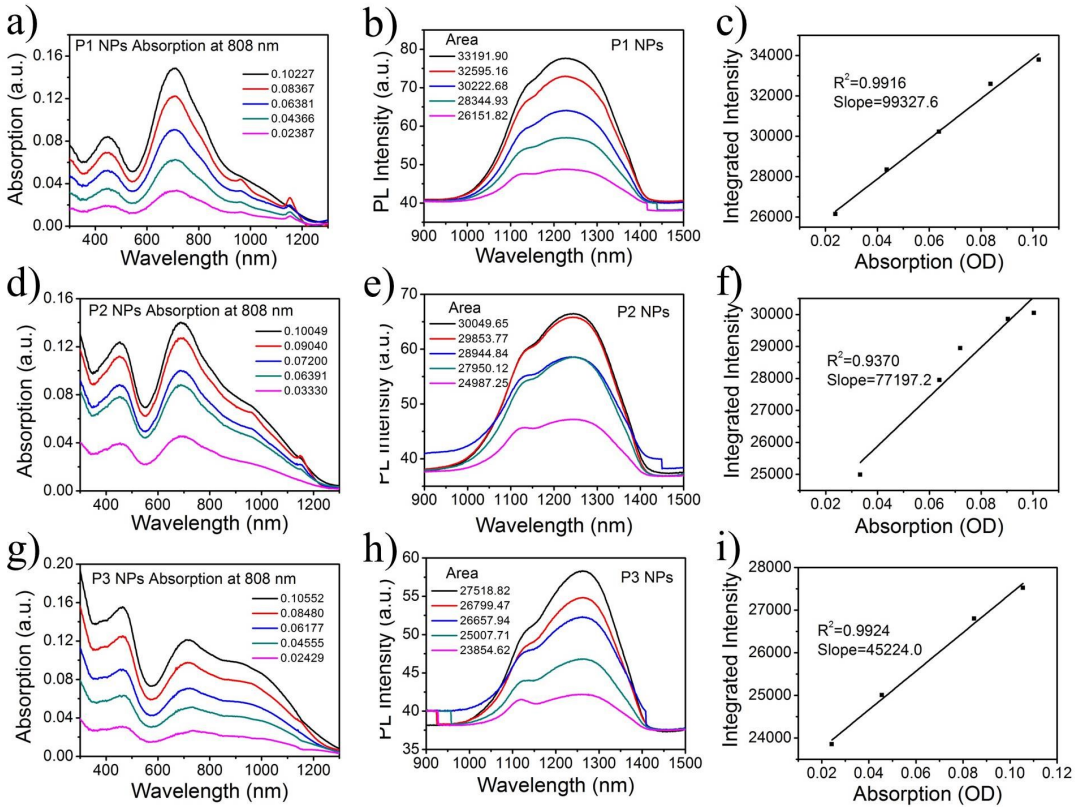

Fig. S7 Fluorescent quantum yield measurement of P1 NPs, P2 NPs, and P3 NPs with IR 1061 as the reference sample. Their corresponding absorption spectrum of (a) P1 NPs, (d) P2 NPs, and (g) P3 NPs in water and IR 1061 in DCM at different absorption. Their corresponding fluorescence emission spectra of (b) P1 NPs, (e) P2 NPs, and (h) P3 NPs in water at different absorption. The plot of the integrated intensity of (c) P1 NPs, (f) P2 NPs, and (i) P3 NPs in water.

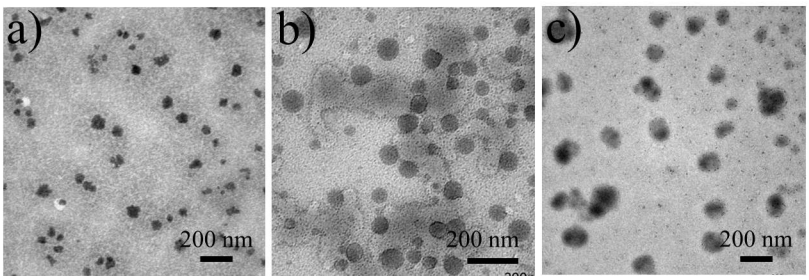

Fig. S8 The TEM images of (a) P1 NPs, (b) P2 NPs, and (c) P3 NPs in water.

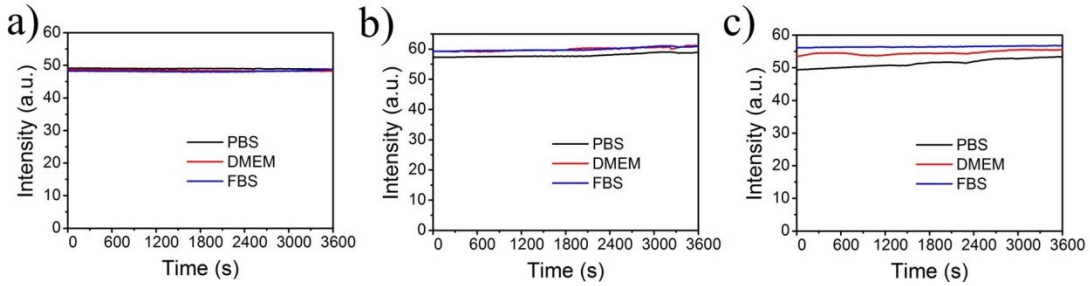

Fig. S9 Photostability test curves of (a) P1 NPs, (b) P2 NPs, and (c) P3 NPs in PBS, DMEM, and FBS under continuous 808 nm laser radiation for 1 h.

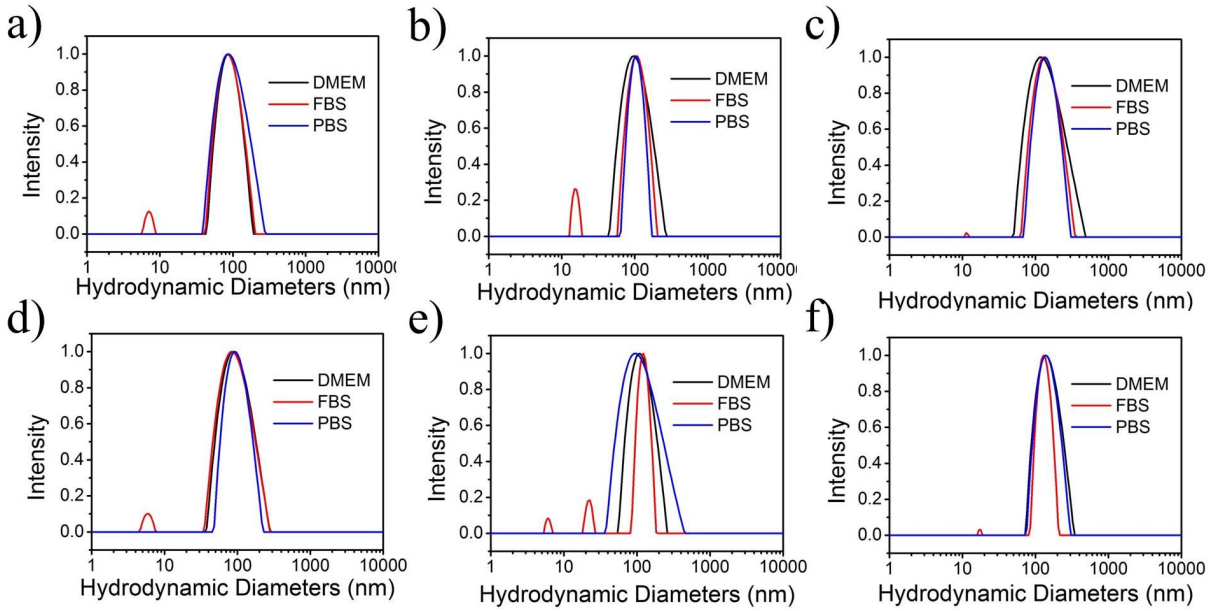

Fig. S10 Hydrodynamic diameters of (a) P1 NPs, (b) P2 NPs, and (c) P3 NPs dispersed in DMEM, FBS and PBS after storage for 24 h, respectively. Hydrodynamic diameters of (d) P1 NPs, (e) P2 NPs, and (f) P3 NPs dispersed in DMEM, FBS and PBS after storage for 7 d, respectively.

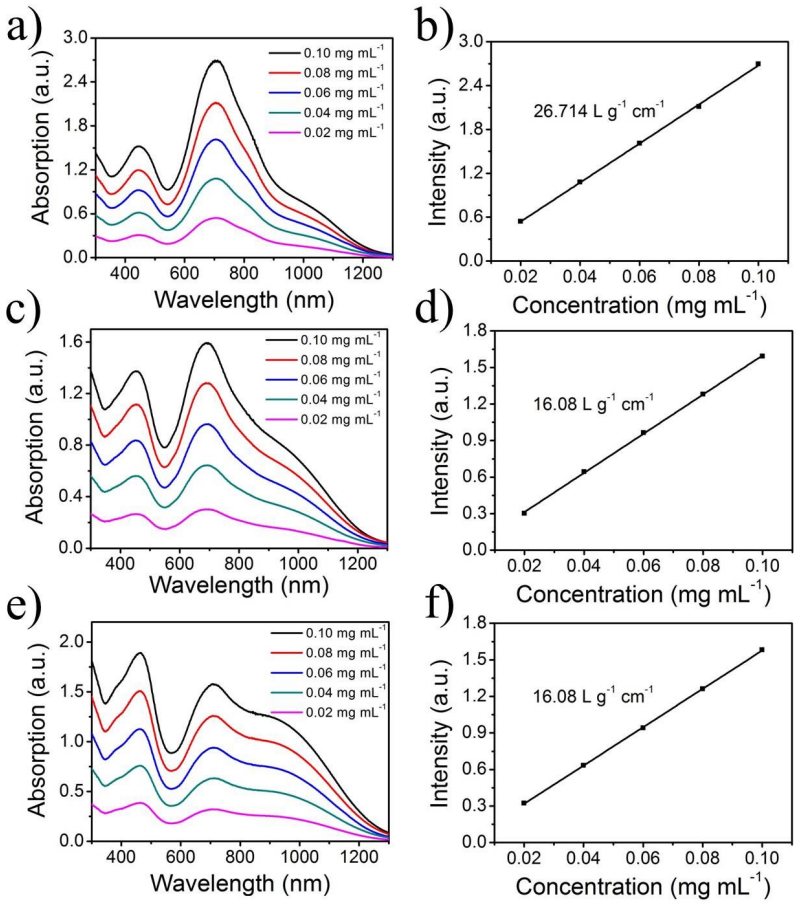

Fig. S11 Photophysical performances of three nanoparticles: UV-vis-NIR absorption spectra of (a) P1 NPs, (c) P2 NPs, and (e) P3 NPs in water at different concentrations. (b), (d) and (f) were their extinction coefficients at their corresponding maximum emission peaks, respectively.

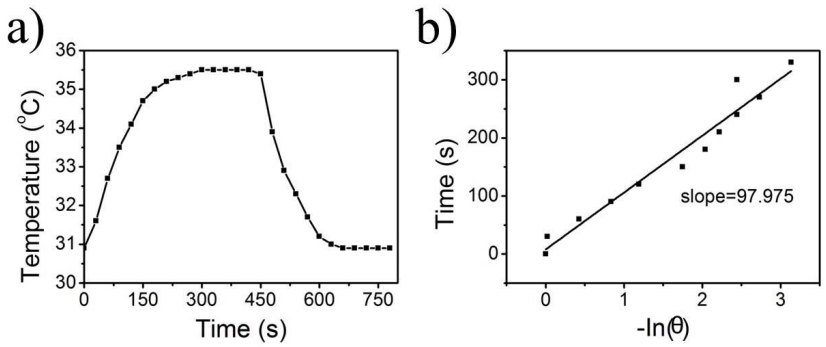

Fig. S12 Photothermal conversion efficiency of deionized water: (a) The photothermal heating and cooling curves of deionized water under the 1064 nm laser irradiation. (b) Linear time data versus negative natural logarithm was obtained from the cooling period.

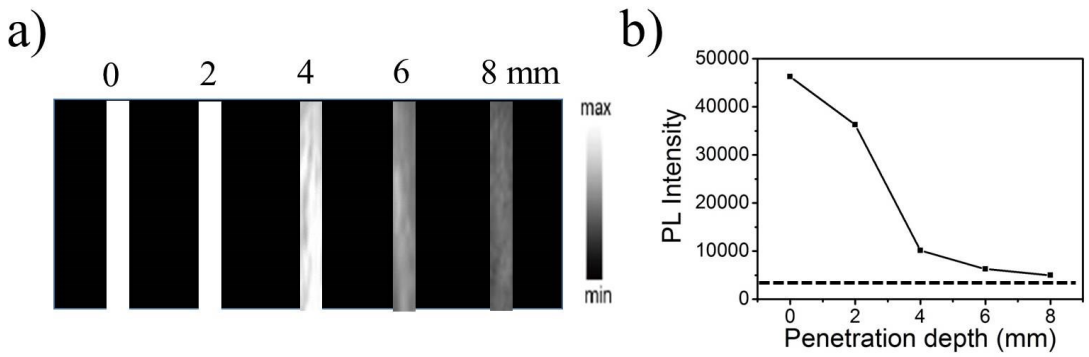

Fig. S13 Penetration depth of P1 NPs: (a) NIR-II fluorescence images of P1 NPs (2 mg mL^{-1}) at different depths under the 808 nm laser excitation (1064 nm LP filter, 500 ms). (b) NIR-II fluorescence intensity of P1 NPs at different depths.

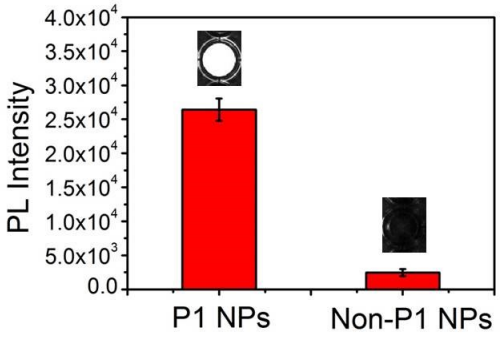

Fig. S14 *In vitro* cellular uptake ability of P1 NPs to 4T1 cells. NIR-II fluorescence images and their corresponding NIR-II Fluorescence signal of the control group (pure 4T1 cells) and 4T1 cells co-incubated with P1 NPs (40 μg mL^{-1}).

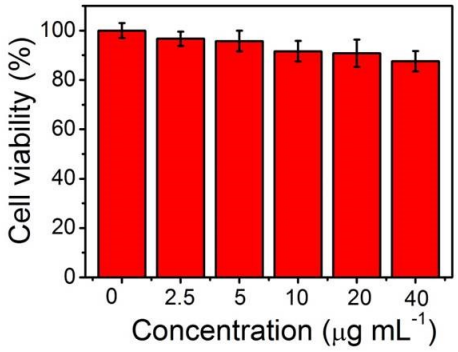

Fig. S15 Cell viabilities of 4T1 cells incubated with P1 NPs at different concentrations without laser for 48 h.

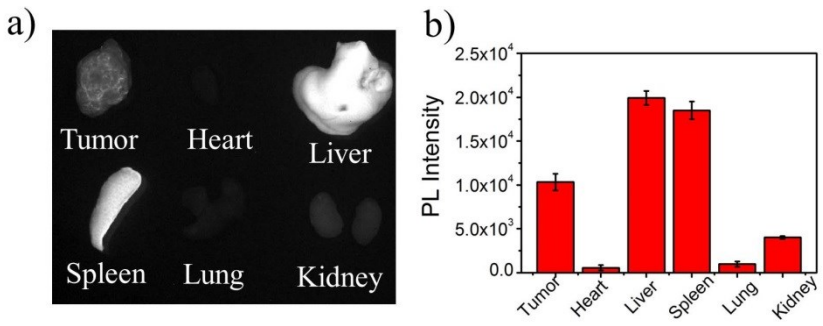

Fig. S16 (a) *In vitro* NIR-II fluorescence images of tumor and major organs (heart, liver, spleen, lung, and kidney) after 48 h of intravenous injection (808 nm laser, 1064 nm LP filter, 500 ms). (b) Quantitative NIR-II fluorescence intensity of tumor and major organs.

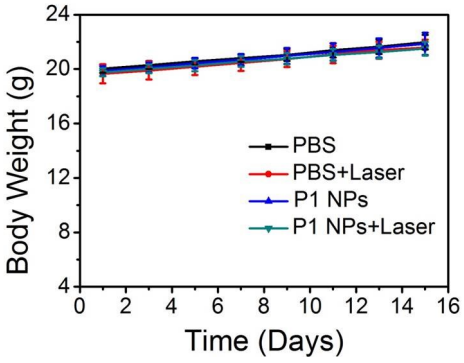

Fig. S17 (a) Changes of body weight with time for different treatment groups.

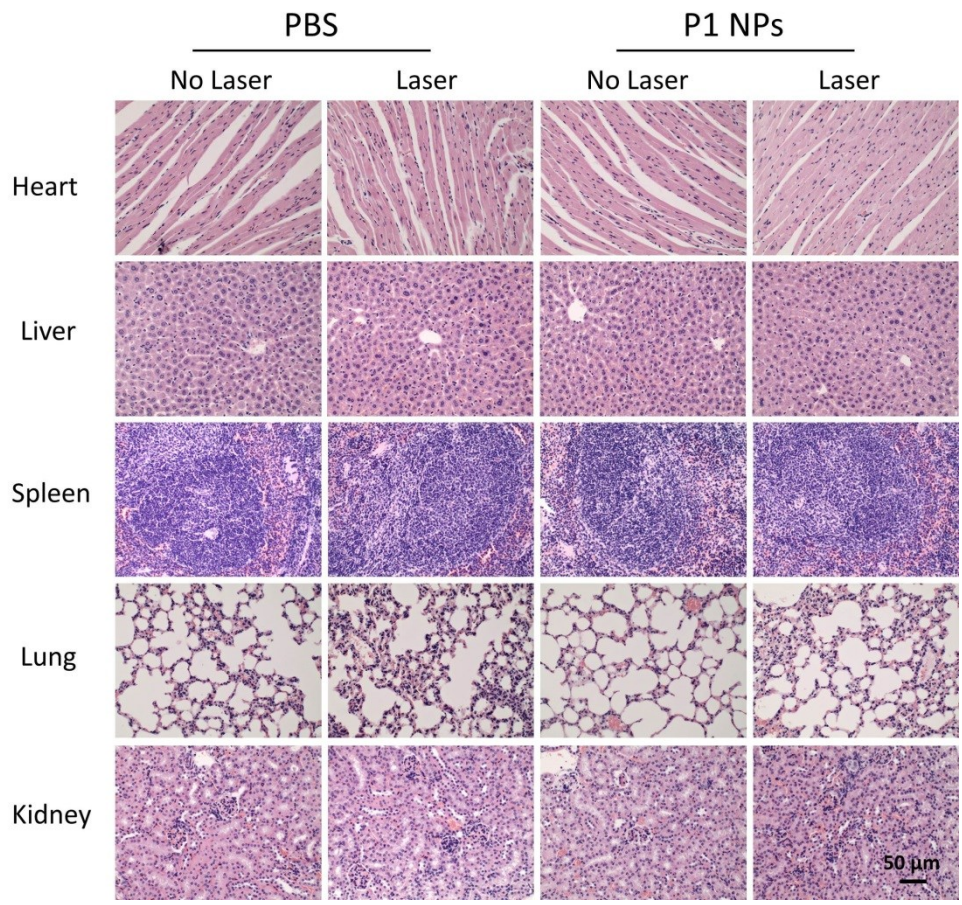

Fig. S18 H&E staining images of organs (heart, liver, spleen, lung, kidney) sections obtained from the four treatment group. Scale bars: 50 μm.